FC

A Publication of

The Metals Research Laboratory

Brown University

Vibration Spectrum And Heat Capacity Of A Chain Polymer Crystal

By

S. M. Genensky and G. F. Newell

Technical Report

Contract No. Nonr-562(08)

Prepared for
Office of Naval Research
Physics Branch
Authority - NR 017-614

April 15, 1956

VIBRATION SPECTRUM AND HEAT CAPACITY OF A CHAIN POLYMER CRYSTAL

By

S. M. Genensky and G. F. Newell

Division of Applied Mathematics

Brown University

Providence 12, Rhode Island

Contract No. Nonr-562(08)

April 15, 1956

Nonr 562-08

Abstract

The Born-von Karman model for a chain polymer crystal previously studied by Stockmayer and Hecht is re-examined using only analytic approximations rather than numerical methods. The analytic approach brings out many peculiar properties of the chain polymer model that did not appear in the numerical treatment.

One branch of the frequency distribution $g(\nu)$ is shown to be proportional to ν^2 for the smallest values of ν, approximately proportional to $\nu^{3/2}$ for slightly larger ν, to $\nu^{1/2}$ for still larger ν and to $\nu^{-1/2}$ in still a fourth range of small values of ν. An accurate graph of $g(\nu)$ is constructed for the entire range of frequencies using values of the force constants suggested by Stockmayer and Hecht. $g(\nu)$ is shown to have approximate singularities of a type not anticipated by van Hove in his broad treatment of singularities for general systems. This anomalous behavior results from having strong valence forces resisting the bending of bond angles. A classification and description of various kinds of singularities that may arise for systems with strong valence forces are given in an appendix.

1. Introduction

The specific heats of lamellar crystals have been the subject of considerable study, both experimental[1] and theoretical[2], in the last few years. Chain polymer or fibrous crystals, on the other hand, have received much less attention despite the fact that they should show anomalies at least as interesting as those of the lamellar crystals.

Stockmayer and Hecht[3] considered a very simple rectangular lattice as a model for a hypothetical chain polymer system and analyzed the spectrum using the numerical scheme of Blackman. The model which they proposed is sufficiently simple, however, that much of the analysis can be done analytically instead of numerically with the result that certain features of the spectrum and of the specific heat that were hidden in the numerical treatment now become more apparent. It is the purpose of the following to extend the analysis of this model and to point out which of these features are representative, at least qualitatively, of a whole class of chain polymer crystals and which features are peculiar to this particular model.

We shall use the same basic notation here as in S-H with the following exception; since we shall be using at all times the reduced force constants and frequencies denoted in S-H by subscripts r, it is convenient to suppress this index. The α, β, $\varkappa$, ν etc. used here shall be interpreted as the α_r, β_r, $\varkappa_r$, ν_r etc. of S-H. The reader is referred to this paper not

only for the notation but for the discussion of the model and the general formulation of the problem. We would like to point out, however, certain significant features in this paper that might otherwise pass unnoticed.

S-H apparently were the first to incorporate into the Born-von Karman model a force constant for bending of valence angles even though it has long been common practice to include such forces in the analysis of the vibrations of complex molecules. The existence of the force constant $\varkappa$ particularly with $\varkappa >> \alpha, \gamma$ is of considerable consequence as will be shown below.

The combination of rectangular geometry and central forces only between chains leads to the result that in Eq. (2.8) of S-H, ν_1^2 (ν_{1r}^2) depends only very weakly upon φ_2 for $\gamma << 1$. This situation also has a pronounced effect upon the spectrum and is in some respects similar to the effect seen in the analysis of the simple cubic crystals[4]: in which second nearest neighbor forces are necessary to prevent the spectrum from becoming essentially one dimensional in form. Any consequences resulting from $\gamma << \alpha$ are closely tied to the rectangular geometry of the crystal and are not to be considered as typical of all chain polymer crystals whereas the consequences of $\varkappa >> \alpha, \gamma$ probably are typical as are also those of $\beta >> \gamma$.

The peculiar effects of the rectangular geometry arise here because for $\gamma = 0$, the normal modes of the system decompose into three branches with the modes for any one branch involving displacements of the particles only along one of the three crystal axes. The modes associated with ν_1^2 are those with

displacement vectors perpendicular to the chains, in the 1 direction. If $\gamma = 0$, the forces resisting displacements in the 1 direction for any given particle arise from the nearest neighbors in the same chain and from the nearest neighbors in those adjacent chains which lie in the 1, 3 plane through this particle. The essential point is that for $\gamma = 0$ there is no coupling between the displacements of this particle in the 1 direction with the displacements in the 1 direction by particles in adjacent 1, 3 planes. Adjacent 1, 3 planes vibrate independently in the 1 direction and so for this branch with $\gamma = 0$, the behavior of the system is really that of a two dimensional array of chains rather than what might be described as a typical three dimensional array. It is this feature of the rectangular lattice which is responsible for the very weak dependence of v_1^2 on φ_2 mentioned above.

Similar arguments apply to the branch represented by v_2^2, except that the role of the 1 and 2 directions are interchanged. For the third branch, v_3^2, the displacements are along the chain. The dominant feature is the strong central force between nearest neighbors in the chain. The nearest neighbor interactions between chains do not appear in v_3^2 because the central forces between such neighbors act only perpendicular to the chain. Any coupling between chains can arise only from the second nearest neighbors and therefore is very weak. That the coupling between chains is relatively weak would be typical of

most chain polymers because of the very strong central forces between adjacent particles in the chain as compared with the forces between chains. However, if the geometry of the lattice were such that nearest neighbors in adjacent chains did not lie in a plane perpendicular to the direction of the chain then the coupling between chains would be proportional to the nearest neighbor force constant (α) instead of the second nearest neighbor force constant (γ).

Our purpose here is to analyze specifically the model as proposed by S-H but it is clear that the peculiar properties of the rectangular lattice are closely connected with the choice of $\gamma \ll \alpha$ and that if γ were not chosen small compared with α, the system would be more typical of chain polymer crystals in general.

2. Vibration Spectrum.

The first problem to consider is that of analyzing the vibration spectrum and the shape of the surfaces of constant frequency in the wave number space (φ_1, φ_2, φ_3). From S-H Eq. (2.8) we note that ν_1^2 and ν_2^2 differ only in that φ_1 and φ_2 are interchanged. If we consider the entire range $0 < \varphi_1, \varphi_2, \varphi_3 < \pi$, then the frequency spectra of the first two branches are identical. The third branch is exactly the same as that of a cubic lattice which has already been considered in some detail[4]. The spectrum of the third branch is plotted in Fig. 5 for the values of the force constants used by S-H. Only the spectrum of ν_1^2 needs special consideration.

The frequencies for this branch are given by S-H, Eq. 2.8

$$\nu_1^2 = (\alpha/2)(1 - \cos\varphi_1) + \gamma(2 - \cos\varphi_1\cos\varphi_2 - \cos\varphi_1\cos\varphi_3) + \varkappa(1 - \cos\varphi_3)^2 \qquad (1)$$

To analyze the shape of the surfaces of constant frequency in the $(\varphi_1, \varphi_2, \varphi_3)$ space, we first inspect the behavior for small ν_1^2. For $\nu_1^2 < \gamma << 1$, it is necessary that the first and last terms of Eq. (1) be small, of order γ or less with $\gamma << \alpha, \varkappa$. This, in turn, requires that φ_1 and φ_3 both be small and so we can expand in powers of φ_1 and φ_3 to obtain

$$\nu_1^2 \sim [(\alpha/4) + (\gamma/2)(1 + \cos\varphi_2)]\varphi_1^2 + \gamma(1 - \cos\varphi_2) + (\gamma/2)\varphi_3^2 + (\varkappa/4)\varphi_3^4 \quad \text{for} \quad \nu_1^2 < O(\gamma) \qquad (2)$$

This includes all terms in the expansion that are necessary to determine the qualitative behavior for $0 < \nu_1^2 < \gamma$.

For sufficiently small ν_1^2, namely for $\nu_1^2 << \gamma^2/4\varkappa \sim 10^{-5}$, it is clear that φ_2 must also be small and that $(\gamma/2)\varphi_3^2 >> (\varkappa/4)\varphi_3^4$ so that we obtain (S-H, Eq. 3.4)

$$\nu_1^2 \sim [(\alpha/4) + \gamma]\varphi_1^2 + (\gamma/2)\varphi_2^2 + (\gamma/2)\varphi_3^2 \quad \text{for} \quad 0 < \nu_1^2 << \gamma^2/4\varkappa \qquad (3)$$

For this lowest range of ν_1, the surfaces of constant ν are flat ellipses with axes $\nu_1[(\alpha/4) + \gamma]^{-\frac{1}{2}}$, $\nu_1(\gamma/2)^{-\frac{1}{2}}$ and $\nu_1(\gamma/2)^{-\frac{1}{2}}$ in the 1, 2 and 3 directions respectively. The first of these is much shorter than the other two for $\alpha >> \gamma$, see Fig. 1. The fact that the surfaces are ellipoidal for sufficiently small ν is a feature characteristic of many three dimensional

systems.

As ν_1^2 increases past $\gamma^2/4\varkappa$, φ_2 remains small compared with one but the term $(\varkappa/4)\varphi_3^4$ comes into prominence and quickly overpowers the term $(\gamma/2)\varphi_3^2$ because of the assumption $\varkappa >> \gamma$. Whereas the φ_1 and φ_2 intercepts of the surfaces of constant ν continue to increase nearly proportional to ν, the φ_3 intercept increases at a slower rate approaching the limit $(\nu_1)^{\frac{1}{2}}(\varkappa/4)^{-\frac{1}{4}}$. The surfaces become elongated in the φ_1 direction as shown in Fig. 1 and we see that (S-H Eq. 3.6) except for the very small values of φ_3,

$$\nu_1^2 \sim [(\alpha/4) + \gamma]\varphi_1^2 + (\gamma/2)\varphi_2^2 + (\varkappa/4)\varphi_3^4 \quad \text{for} \quad \gamma^2/4\varkappa << \nu_1 << \gamma \tag{4}$$

This form of ν_1^2 reflects the influence of the strong valence forces with a φ_3 dependence characterized by a fourth power term rather than the more familiar quadradic dependence as in Eq. 3.

As ν_1^2 approaches the value γ, the expansion in powers of φ_2 breaks down and we must go back to Eq. (2) which tells us that for $\nu^2 = 2\gamma$, the surfaces of constant ν pass through a corner of the Brillouin zone at $(0, \pi, 0)$ creating a saddle point such as discussed by van Hove[5]. The surface $\nu_1^2 = 2\gamma$ is one of the surfaces shown in Fig. 2. However, we shall pass over this critical range of ν for the moment.

There follows another region of frequencies $\gamma << \nu_1^2 << \alpha$ in which the γ terms of Eq. (1) are of only minor importance. As can be seen from Fig. 2, the surfaces of constant frequency are nearly independent of φ_2 (cylinders) with

the γ terms only causing a ripple in the surface. In this range of ν_1, φ_3 is still small and except for the very smallest values of φ_3,

$$\nu_1^2 \sim (\alpha/2)(1 - \cos \varphi_1) + (\varkappa/4)\varphi_3^4 \qquad \text{for } \gamma \ll \nu_1^2 < \alpha \tag{5}$$

The extent to which such a range of frequencies exists depends upon the validity of the condition $\alpha \gg \gamma$. Such a condition is a consequence of the rectangular geometry, not simply of the fibrous structure.

As ν_1^2 approaches the value α, the surfaces come close to an edge of the Brillouin zone and the detailed shape near this edge becomes sensitive to the γ terms of Eq. 1. We shall pass over this critical range also for the moment and consider still larger values of ν_1^2.

For $\alpha \ll \nu^2 \ll 4\varkappa$, the α terms of Eq. (1) as well as the γ terms become relatively unimportant but φ_3 is no longer small. ν_1^2 is nearly independent of both φ_1 and φ_2; the surfaces of constant ν_1 are nearly planes with

$$\nu_1^2 \sim \varkappa(1 - \cos \varphi_3)^2 \qquad \text{for} \qquad \alpha \ll \nu^2 < 4\varkappa \tag{6}$$

As ν_1^2 approaches the value $4\varkappa$, the surfaces approach a face of the zone and the dependence of ν_1^2 on α and γ once again comes into prominence. Figure 2 shows some of these surfaces of constant ν, particularly those which pass near and through critical points of the Brillouin zone. Because of the very small value of γ, some of the details of the surfaces can not

be shown on a figure of this scale particularly the behavior of the surfaces passing near the two corners $(\pi, \pi, 0)$ and $(\pi, 0, 0)$.

The critical values of the frequency which were passed over in the above description give rise to singularities in the frequency distribution to be discussed in the next section. These are associated with stationary values of ν_I^2 considered as a function of φ_1, φ_2 and φ_3 and can be found analytically from Eq. (1) by determining those values of $(\varphi_1, \varphi_2, \varphi_3)$ and ν_I^2 for which $\partial\nu_I^2/\partial\varphi_j = 0$, $j = 1, 2, 3$. These critical values are listed in Table I.

From the signs of the second derivatives, one also determines whether any such point represents a maximum, minimum or a saddle point of ν_I^2. The saddle points are decomposed into two categories denoted by S.P.I and S.P.II. For S.P.I, the surfaces of constant ν are two sheeted for frequencies below the critical frequency ν_c and one sheeted above the critical frequency. S.P.II differs only in that the order is reversed; the surfaces are two sheeted for frequencies above the critical frequency and one sheeted below. This distinction shows up in the frequency distribution $g(\nu)$ in that for type I saddle points there is a verticle tangent singularity as $\nu \rightarrow \nu_c$ from the left whereas for type II, the verticle tangent singularity appears as $\nu \rightarrow \nu_c$ from the right.

Table I. The critical points of the vibration spectrum for ν_1 are listed below. The first column gives the point $(\varphi_1, \varphi_2, \varphi_3)$ of the wave vector space and column two the frequency at these points. The third column gives the type of singularity. Max denotes local maximum, min, minimum whereas S.P.I and S.P.II represent two types of saddle points.

$(\varphi_1, \varphi_2, \varphi_3)$	ν_1^2	Type
$(0, 0, 0)$	0	min.
$(0, \pi, 0)$	2γ	S.P.I
$(\pi, \pi, \cos^{-1}(1 - \gamma/2\varkappa))$	$\alpha + 2\gamma - \gamma^2/4\varkappa$	S.P.I
$(\pi, \pi, 0)$	$\alpha + 2\gamma$	S.P.II
$(\pi, 0, \cos^{-1}(1 - \gamma/2\varkappa))$	$\alpha + 4\gamma - \gamma^2/4\varkappa$	S.P.II
$(\pi, 0, 0)$	$\alpha + 4\gamma$	max.
$(0, 0, \pi)$	$4\varkappa + 2\gamma$	S.P.I
$(0, \pi, \pi)$	$4\varkappa + 4\gamma$	S.P.II
(π, π, π)	$4\varkappa + \alpha$	S.P.II
$(\pi, 0, \pi)$	$4\varkappa + \alpha + 2\gamma$	max.

It is interesting to note that there are more than the minimum number of critical points (10 instead of 8). In addition to the expected singularities at corners of the Brillouin zone, there are also two saddle points at $(\pi, 0, \cos^{-1}(1-\gamma/2\varkappa))$ and at $(\pi, \pi, \cos^{-1}(1 - \gamma/2\varkappa))$. Furthermore the singularity at the corner $(\pi, 0, 0)$ is a local maximum.

Two of these singularities lie very close to the corners with $\varphi_3 \sim (\gamma/\varkappa)^{\frac{1}{2}} \ll 1$. The frequencies at these points are extremely close to the corresponding frequencies at the corner, the values of ν^2 differing by only $\gamma^2/4\varkappa \sim 10^{-5}$. Such details are poorly resolved in Fig. 2 and do not appear at all in the spectrum plotted in Fig. 4. The fact that there are two singularities with frequencies very close together is of little physical importance in itself; it is of interest here mainly because we shall note in Sec. 4 that as the two singularities coalesce into one for $\gamma \longrightarrow 0$, a singularity in the distribution of a slightly different type results.

3. The Frequency Distribution

In view of the complexity of the frequency spectrum Eq. (1), there seems little hope of evaluating exactly the frequency distribution function $g_1(\nu)$ of the first branch from the definition

$$g_1(\nu) = \frac{2\nu}{\pi^3} \frac{d}{d\nu^2} \iiint d\varphi_1 d\varphi_2 d\varphi_3 \qquad (7)$$

with the integral evaluated over the range

$$0 \leq \nu_1^2(\varphi_1, \varphi_2, \varphi_3) \leq \nu^2$$

and

$$0 \leq \varphi_i \leq \pi \qquad i = 1, 2, 3$$

It is possible, however, to obtain quantitatively accurate approximations to $g_1(\nu)$ over certain ranges of ν based upon the approximations used in Eqs. (2) and (6).

By substituting Eq. (3) into Eq. (7), one finds very easily that[6].

$$g_1(\nu) \sim 2\pi^{-2}\gamma^{-1}(\alpha + 4\gamma)^{-\frac{1}{2}}\, \nu^2 \mathfrak{d}\nu^2 \qquad \text{for} \qquad 0 < \nu^2 << \gamma^2/4\varkappa \tag{8}$$

The quadratic dependence of $g_1(\nu)$ on ν is typical of all three dimensional systems and, as we shall see, gives the usual Debye T^3 -law for the specific heat. The distinguishing feature of Eq. (8) is the fact that this relation holds only over a very short range of ν as compared with non-fibrous crystals.

From Eq. (4) we find that

$$g_1(\nu) \sim 2\pi^{-2}\gamma^{-\frac{1}{2}}(\alpha + 4\gamma)^{-\frac{1}{2}}\varkappa^{-\frac{1}{2}}\nu^{3/2}\mathfrak{d}\nu^{3/2} \qquad \text{for} \quad \gamma^2/4\varkappa << \nu^2 << \gamma \tag{9}$$

As noted also in Eq. (4), this form arises because at these frequencies the valence forces have become the dominant influence in the φ_3 direction. The $\nu^{3/2}$ dependence is a feature that is expected to be more or less typical of chain polymer crystals.

Actually by combining terms in Eq. (3) and (4), it is possible to obtain an approximation valid over the entire range $0 < \nu^2 << \gamma$ for which the above are just limiting cases.

$$g_1(\nu) \sim 2^{\frac{1}{2}}\pi^{-2}(\alpha + 4\gamma)^{-\frac{1}{2}}\gamma^{-\frac{1}{2}}\nu\left\{[(\gamma/\varkappa)^2 + 4\nu^2/\varkappa]^{\frac{1}{2}} - \gamma/\varkappa\right\}^{\frac{1}{2}}$$

$$\text{for} \quad 0 < \nu^2 \ll \gamma \qquad (10)$$

Equation (10) is plotted as the solid curve of Fig. 3 and the two limiting equations, Eqs. (8), (9) are shown by the broken lines. The range of frequencies involved here is very low and the whole of Fig. 3 is a greatly magnified (about 40 to 1) view of the small rectangle near the origin of Fig. 4.

If we pass over the region around $\nu^2 = 2\gamma$ for the moment and go to slightly higher frequencies, we come to a range where Eq. (5) holds. Despite its simple form, Eq. (5) does not yield elementary integrals, but leads to the form

$$g_1(\nu) \sim \pi^{-2}\varkappa^{-\frac{1}{2}}\sqrt{2}\int_0^{\varphi_m} d\varphi_1[\nu^2 - \alpha\sin^2(\varphi_1/2)]^{-3/4} \qquad (11a)$$

in which φ_m is the value of φ_1 for which $\nu^2 = \alpha\sin^2(\varphi_1/2)$.

If we let $y = \alpha\nu^{-2}\sin^2(\varphi_1/2)$, Eq. (11a) gives

$$g_1(\nu) \sim 2^{-\frac{1}{2}}\pi^{-2}\varkappa^{-\frac{1}{2}}(\alpha + 2\gamma)^{-\frac{1}{2}}\nu^{\frac{1}{2}}\int_0^1 dy\, y^{-\frac{1}{2}}(1 - y)^{-3/4}(1 - \nu^2 y/\alpha)^{-\frac{1}{2}} \qquad (11b)$$

and if we restrict ν^2 so that $\nu^2 \ll \alpha$, the integral can be evaluated in a power series in ν^2/α of which the leading term is

$$g_1(\nu) \sim \tfrac{1}{2}\ \pi^{-5/2}\alpha^{-\frac{1}{2}}\varkappa^{-\frac{1}{2}}[\Gamma(\tfrac{1}{4})]^2\ \nu^{\frac{1}{2}}d\nu^{\frac{1}{2}} \quad \text{for} \quad 2\gamma \ll \nu^2 \ll \alpha \qquad (12)$$

Γ is the gamma function which can also be expressed in terms of complete elliptic integrals through the relation $[\Gamma(\frac{1}{4})]^2 = 4\sqrt{\pi}\,K(2^{-\frac{1}{2}})$.

We could also have obtained Eq. (12), by restricting the

range of φ_1 in Eq. (5) and replacing cos φ_1 by $1 - \varphi_1^2/2$.

The $\nu^{1/2}$ dependence results from having cylindrical wave surfaces with one intercept proportional to $\nu^{1/2}$ and the other proportional to ν and as noted in Eq. (5), this feature is mainly due to the rectangular geometry. With a value of $\alpha/2\gamma$ of only about 10, the existence of a well defined frequency range with $2\gamma << \nu^2 << \alpha$ may be questioned even for the values of the constants used here. If, however, we could make this ratio appreciably larger such a range would certainly exist.

A plot of Eq. (12) is shown in Fig. 4 as one of the broken lines. It is seen to give only a fair approximation over a quite limited range and for these values of the constants, the more accurate curve shown by the solid line would hardly be recognized as being proportional to $\nu^{1/2}$.

If we consider next the region of still higher frequencies where $\alpha << \nu_1^2 < 4\varkappa$, we can use Eq. (6) which again yields a simple expression for $g_1(\nu)$

$$g_1(\nu) \sim 2^{-\frac{1}{2}}\pi^{-1}\varkappa^{-\frac{1}{2}}[1 - (\nu^2/4\varkappa)^{\frac{1}{2}}]^{-\frac{1}{2}}\nu^{-\frac{1}{2}} \quad \text{for} \quad \alpha << \nu^2 < 4\varkappa \tag{13}$$

which actually gives a fairly good approximation over most of the range from α to $4\varkappa$. This equation is not shown in Fig. 4 but the solid curve shown is obtained from a power series expansion in $(\alpha/\varkappa)$ that converges quite rapidly over most of this range. Equation (13) is the lowest term of this expansion.

It is interesting to note that from Eq. (13), we can obtain another limiting form

$$g_1(\nu) \sim 2^{-\frac{1}{2}}\pi^{-1}\varkappa^{-\frac{1}{2}}\nu^{-\frac{1}{2}}\alpha\,\nu^{-\frac{1}{2}} \qquad \text{for} \qquad \alpha \ll \nu^2 \ll 4\varkappa \qquad (14)$$

Again for the choice of constants used here with $4\varkappa/\alpha \sim 10$, the existence of any such frequency range is questionable. A plot of Eq. (14) is shown in Fig. 4 where one may see that this approximation is not particularly good. The $\nu^{-\frac{1}{2}}$ dependence of $g(\nu)$ does, however, represent a limiting situation in which $4\varkappa/\alpha >> 1$ and would indeed be recognized if we could make this ratio appreciably larger than just 10.

This frequency dependence is not simply a result of geometry. Similar results would also be obtained for $\varkappa >> \alpha, \gamma$ without any assumptions regarding the relative size of α and γ. It is a consequence of the choice of the valence forces as the dominant influence for the modes vibrating perpendicular to the chain and is likely to be typical of any chain polymer crystal.

It is worth noting perhaps at this time that some of the approximations discussed so far work very well and others are rather crude even though the assumption $\alpha/2\gamma \sim 10 >> 1$ and $4\varkappa/\alpha \sim 10 >> 1$ seems quite reasonable. The reason for this is that the errors are in some cases proportional to $(2\gamma/\alpha)^{\frac{1}{2}}$ or $(\alpha/4\varkappa)^{\frac{1}{2}} \sim \frac{1}{3}$ or even $(\alpha/4\varkappa)^{\frac{1}{4}} \sim \frac{1}{1.7}$ rather than $(\alpha/4\varkappa) \sim \frac{1}{10}$. For example, we may say that φ_3 is small in Eq. (5) when $\nu^2 \sim \alpha << \varkappa$ but actually φ_3 is of order $(4\alpha/\varkappa)^{\frac{1}{4}}$ which really is not very small; in fact it is very nearly 1. It is not surprising then that the approximations in Fig. 4 are not accurate to the order of 10% as might be expected from a hasty judgment. Indeed such things as effective Debye temperatures

and other qualitative measures of the sizes of physical constants are really proportional to frequencies which in turn are proportional to square roots of force constants rather than the force constants themselves.

On the basis of the analysis so far, we see, however, that for an extreme situation in which $\gamma \ll \alpha \ll \varkappa$, the frequency distribution $g_1(\nu)$ varies as ν^2 at the lowest frequencies, gradually changes over to a $\nu^{3/2}$ dependence starting at ν^2 in the vicinity of $\gamma^2/4\varkappa$, later goes over to a $\nu^{1/2}$ dependence when ν^2 becomes larger than γ and finally varies as $\nu^{-\frac{1}{2}}$ after ν^2 becomes larger than α but still small compared with $4\varkappa$. The effects of this on the specific heat will be shown in Sec. 5.

The problem of actually constructing an accurate graph of $g_1(\nu)$ for the entire range of ν, is a rather tedious job. For each of the frequency ranges considered above, the approximate formulae for $g_1(\nu)$ can be used as first approximations and more accurate expressions obtained by expansions in powers of γ/α, $\alpha/\varkappa$ (fractional powers in most cases) or whatever may be appropriate, depending upon what has been neglected in Eq. (1), to arrive at the lowest approximation. Such a procedure was used to obtain the solid curve of Fig. 4 in the appropriate ranges. The formulae and detailed procedures for this are fairly straightforward and not sufficiently interesting to warrant presentation here. Suffice it to note that this procedure is not a satisfactory one for obtaining $g_1(\nu)$ near its singularities where the expansions will converge very slowly

if at all. The regions considered by this method are non-overlapping and give little information regarding $g_1(\nu)$ for ν^2 near the values 2γ, α or $4\varkappa$.

4. Singular points

Van Hove[5] has described the analytic form of the singular points for any quite general two or three dimensional crystalline lattice. This description can indeed be applied to the present problem but it really does not tell the whole story. Highly anisotropic crystals, in general, and the present model in particular with strong valence forces give rise to anomalous behaviors near many of the singular points as illustrated, for example, in Fig. 4 at the point $\nu^2 = \alpha$. This singularity, though actually having a verticle tangent only on one side of the singular point, appears more like a true cusp with a verticle tangent on both sides of the singularity.

We have already seen that the strong valence forces cause unusual behavior near the origin, the minimum point of the spectrum, which is in a certain sense one of the singularities. Also we have seen that for ν^2 near $\alpha + 2\gamma$ and also for ν^2 near $\alpha + 4\gamma$, there are two singularities so close together that it would be impossible to resolve them on a scale of frequencies such as that used in Fig. 4.

Table I lists all the singular points. By expansion of ν^2 as given by Eq. (1) about the critical values of φ_1, φ_2, φ_3 one can easily deduce in accordance with van Hove that near any critical frequency ν_c, except $\nu = 0$, $g(\nu)$ has the general form

$$g(\nu) = a + b \text{ Real } [\pm (\nu - \nu_c)]^{\frac{1}{2}} + O(\nu - \nu_c) \qquad (15)$$

The $\pm$ sign inside the square root and the sign of b are chosen in accordance with the four types of singularities as listed in Table I. b is negative for S.P.I and S.P.II, positive for max. and min. The + sign is chosen for S.P.II and min., the - sign for S.P.I and max. The values of the constant b is determined easily from values of the second derivative of ν^2 with respect to the φ's at the critical φ's. The value of the constant a does not usually depend only upon the local properties of ν^2 near the critical φ's, however, and is not so easily determined explicitly.

The origin $\nu = 0$ does not give a singularity in $g(\nu)$ but there is a vertical tangent singularity in

$$G(\nu^2) = (2\nu)^{-1} g(\nu) \qquad (16)$$

the distribution of values of ν^2. In place of Eq. (15) we find for $G(\nu^2)$ the analogous form

$$G(\nu^2) = A + B \text{ Real } [\pm (\nu^2 - \nu_c^2)]^{\frac{1}{2}} + O(\nu^2 - \nu_c^2) \qquad (17)$$

at every critical frequency ν_c including $\nu = 0$.

The behavior of $G(\nu^2)$ near the origin indicates to a certain extent the type and cause of anomalies in $G(\nu^2)$ and $g(\nu)$ at some of the other critical points.

From Eq. (8) and Eq. (16), we see that $G(\nu^2)$, considered as a function of ν^2, starts out at $\nu = 0$ with

$$G(\nu^2) \propto \nu = (\nu^2)^{\frac{1}{2}} \qquad \text{for } 0 < \nu^2 \ll \gamma^2/4\varkappa \qquad (18)$$

in agreement with the general form Eq. (17) with A = 0 (as it must be for an absolute minimum).

ν^2 has a complete range of order 1 whereas Eq. (18) holds only for $\nu^2 \ll \gamma^2/4\varkappa \sim 10^{-5}$. This behavior is confined to such a small range that it would not be resolved on any graph showing the whole spectrum $G(\nu^2)$ vs. ν^2; it did not even show on the graph of $g(\nu)$ vs. ν which is relatively much more sensitive to the behavior near $\nu = 0$.

As soon as the valence forces come into prominence with the characteristic dependence of ν^2 on φ_3^4, $g(\nu) \propto \nu^{3/2}$ and

$$G(\nu^2) \propto \nu^{\frac{1}{2}} = (\nu^2)^{\frac{1}{4}} \qquad \text{for } \gamma^2/4\varkappa \ll \nu^2 \ll 2\gamma \qquad (19)$$

The singularity has changed from a square root type to a fourth root. Although this formula is also confined to a very small scale of ν^2 values, $\nu^2 \ll 4 \times 10^{-3}$, it is this feature which is of particular interest for it is one of several possible types of singularities that arise when ν^2 has a stationary value with a local dependence upon the wave numbers that is quadratic in some directions (φ_1 and φ_2) but primarily fourth power in other directions (φ_3). This feature is characteristic of all the singularities that lie on or near the face $\varphi_3 = 0$ in this particular problem. It is a feature that is not peculiar to this particular model but will arise in most any model having strong valence forces with the characteristic fourth power dependence of ν^2 on one or more of the wave numbers.

The fourth root singularity is typical of any system in which ν^2 behaves locally as

$$\nu^2 = \nu_c^2 + a(\varphi_1 - \varphi_{1c})^2 + b(\varphi_2 - \varphi_{2c})^2 + c(\varphi_3 - \varphi_{3c})^4 \qquad (20)$$

in which ν_c is a critical frequency, a, b, c are positive constants and $(\varphi_{1c}, \varphi_{2c}, \varphi_{3c})$ is a critical wave vector.

Because of the rectangular geometry and the fact that this model degenerates into a two dimensional problem with $\gamma \longrightarrow 0$, we have an illustration here of still another type of singularity. Equation (5) for $\varphi_1 << 1$ represents a two dimensioanl form of Eq. (20), b = 0, and as we have already seen $g(\nu) \propto \nu^{3/2}$ and

$$G(\nu^2) \propto \nu^{-\frac{1}{2}} = (\nu^2)^{-\frac{1}{4}} \qquad \text{for } 2\gamma << \nu^2 << \alpha \qquad (21)$$

The negative fourth root singularity is typical of the two dimensional form of Eq. (20).

On still a larger scale of ν^2, Eq. (6) with $\varphi_3 << 1$ represents a one dimensional form of Eq. (20) with a = b = 0 and $g(\nu) \propto \nu^{\frac{1}{2}}$

$$G(\nu^2) \propto \nu^{-3/2} = (\nu^2)^{-3/4} \qquad \text{for } \alpha << \nu^2 << 4\pi \qquad (22)$$

The negative three-fourths powers singularity is representative of the one dimensional form of a minimum having a fourth power dependence of ν^2 on φ_3.

If now we go on to the singularity at $\nu^2 = 2\gamma$, we do indeed see that in the immediate vicinity of $(0, \pi, 0)$, there is

a singularity of standard type (S.P.I) but since it is on the face $\varphi_3 = 0$, the dependence of ν^2 on φ_3 is to a large extent dominated by the fourth power term. ν^2 behaves approximately as given in Eq. (20) but with a negative value of b. We have a "singular" type of saddle point.

On the scale with which Fig. 4 is drawn, only the behavior typical of the singular type of saddle point can be shown. We have included in the appendix a discussion of all the possible types of singularities that might arise from valence forces. It is shown there that this type of saddle point gives rise to a fourth root verticle tangent singularity in $g(\nu)$ on both sides of ν_c (not necessarily symmetric about ν_c, however). This explains why $g(\nu)$ appears to have a true cusp at $\nu^2 = 2\gamma$.

It has been possible to actually obtain, explicitly, accurate analytic approximations for $g(\nu)$ everywhere including all the singular points. Unfortunately the derivation of these expressions involves using slightly different techniques at each of the singular points depending upon which of the many variables involved in the integrations may be small for any particular value of ν. The results are not exactly trivial and in most cases involve combinations of Γ-functions. It would not be possible to describe all the various approximations here. Mainly as an illustration of the form of a typical result we give below an approximation for $g(\nu)$ which is fairly accurate in a small region near the point $\nu^2 = 2\gamma$

$$g(\nu) = \frac{[\Gamma(1/4)]^4 \gamma^{\frac{1}{2}}}{2(\alpha + 2\gamma)^{\frac{1}{2}}\pi^4(2\varkappa)^{\frac{1}{2}}}\left\{1 - \frac{8\pi^2\sqrt{2}}{[\Gamma(1/4)]^4}\ \text{Real}\left(\frac{-\nu^2 + 2\gamma}{2\gamma}\right)^{1/4}\right\}$$

$$\text{for } 10^{-3} \sim \gamma/16\ \varkappa << |-1 + \nu/\sqrt{2\gamma}| << 1$$

This formula does not apply at the singular point itself because, strictly speaking, there is no verticle tangent on both sides of the singularity but it would be necessary to draw a graph that shows frequency differences of order $\sqrt{2\gamma}\ \gamma/16\ \varkappa \sim 10^{-4}$ to see this.

The behavior near $\nu^2 \sim \alpha$ is even more unusual. Near the point $(\pi, \pi, 0)$, $\nu^2 \sim \alpha + 2\gamma$, there are two singularities. This results because near this point the dependence of ν^2 on φ_3 is represented by a negative but small (proportional to γ) quadratic term plus a positive but large (proportional to $\varkappa$) fourth power term. As a function of φ_3, ν^2 has a minimum resulting from the competing influences of the quadratic and fourth power terms. In addition to the stationary value of ν^2 at $\varphi_3 = 0$ there is a second stationary value a short distance away from the corner. This anomaly is at least indicated in Fig. 2 but the double singularity cannot be resolved in Fig. 4. Figure 4 shows only the influence of the fourth power φ_3 terms but not the quadratic terms. Disregarding this fine structure, the behavior of ν^2 is described by an equation of the type Eq. (20) with $a < 0$ and $b, c > 0$. This gives another singular saddle point of exactly the same type as at $\nu^2 = 2\gamma$ with approximately verticle tangents for $g(\nu)$ on both sides of the point $\nu^2 = \alpha + 2\gamma$.

At the point $(\pi, 0, 0)$, $\nu^2 \sim \alpha + 4\gamma$, we have a similar situation with a pair of singular points due to the same sort of dependence of ν^2 on φ_3. The exact picture is somewhat more complicated than at the point $(\pi, \pi, 0)$ because of the creation at the corner of a local maximum and an "island" by the saddle point a short distance away from the corner. Figure 4 is, however, again drawn on too coarse a scale to show this and near this corner the frequencies are given approximately by Eq. (20) with $a, b < 0$ and $c > 0$. Although this is also a singular saddle point, it is not of the same type as those at $\nu^2 = 2\gamma$ and $\nu^2 = \alpha + 2\gamma$ by virtue of the fact that both quadratic terms (a and b) are negative at $\nu^2 = \alpha + 4\gamma$ whereas at the other two frequencies only one of these terms is negative. It is shown in the appendix that this new type of saddle point gives rise to an infinite discontinuity in slope with a finite slope on one side (in this case the low frequency side of ν_c) and a vertical tangent on the other side. In this respect it is the same sort of behavior as obtained from a saddle point of standard type but the verticle tangent arises in the present instance from a fourth root rather than a square root singularity.

The fact that for $\gamma << 1$ all singular points at $\nu^2 = \alpha + 2\gamma$ and $\nu^2 = \alpha + 4\gamma$ lie very close together indicates that on a coarse scale of frequencies in which frequency differences of order γ are not resolved, the $g(\nu)$ curve has an approximate singularity of still another kind in the vicinity of $\nu^2 = \alpha$. This is, of course, due to the fact that for

$\gamma \longrightarrow 0$, the problem reduces to a two dimensional problem and as a two dimensional problem, the surfaces of constant ν are all cylinders independent of φ_2 with the line $(\pi, \varphi_2, 0)$ a line of singularities.

The form of the surfaces of constant frequency is represented approximately by Eq. (20) with $b = 0$, $a < 0$, $c > 0$, a singular form of a two dimensional saddle point. In the appendix it is shown that this gives rise to an infinite singularity of the type

$$g(\nu) \propto \text{Real } (\nu_c - \nu)^{-\frac{1}{4}} = \begin{cases} (\nu_c - \nu)^{-\frac{1}{4}} & \text{for } \nu_c > \nu \\ 2^{-\frac{1}{2}}(\nu - \nu_c)^{-\frac{1}{4}} & \text{for } \nu_c < \nu \end{cases}$$

Although $g_1(\nu)$ has a minus one fourth power singularity on both sides of ν_c, $g_1(\nu)$ is not symmetric about ν_c. Figure 4 clearly shows the tendency to approximate this two dimensional behavior for $\nu^2 \sim \alpha$.

The remaining singularities of the spectrum all occur on the face $\varphi_3 = \pi$ and are of a more conventional variety although we can again see the effects of having a spectrum that on a very coarse scale tries to approximate a one dimensional spectrum, on a finer scale a two dimensional spectrum and finally the three dimensional spectrum on a still finer scale. We no longer have a local fourth power dependence of ν^2 on the wave numbers near singularities as is true on the face $\varphi_3 = 0$.

The curve clearly shows the usual varieties of verticle tangent singularities characteristic of any three dimensional

system at the four points $\nu^2 = 4\varkappa + 2\gamma$, $4\varkappa + 4\gamma$, $4\varkappa + \alpha$ and $4\varkappa + \alpha + 2\gamma$ which arise from the stationary values of ν^2 at the four corners of the cube on the faces $\varphi_3 = \pi$. On a scale in which frequency differences of order γ are not resolved, the singularities coalesce in pairs at the approximate points $\nu^2 = 4\varkappa$ and $\nu^2 = 4\varkappa + \alpha$. In this approximation the spectrum is two dimensional with the usual two dimensional singularities, a logarithmic singularity at $\nu^2 = 4\varkappa$ coming from the edge $(0, \varphi_2, \pi)$ of Fig. 2 and a discontinuity at the maximum frequency $4\varkappa + \alpha$ coming from the edge (π, φ_2, π) of Fig. 2. This tendency of Fig. 4 to approximate this behavior is clearly indicated.

On a still coarser scale of frequency, all four singularities occur at approximately the same frequency, $\nu^2 \sim 4\varkappa$ and the spectrum approximates that of a one dimensional system with the characteristic recriprocal square root singularity in $g(\nu)$ due to the maximum on the face of the cube $(\varphi_1, \varphi_2, \pi)$. This tendency is illustrated in Fig. 4 by the fact that $g_1(\nu)$ rises quite rapidly as $\nu^2 \longrightarrow \varkappa$ on a coarse scale of frequency.

The fact that it is possible actually to construct a fairly accurate curve for $g_1(\nu)$ throughout the whole range of ν is to a large extent a consequence of the fact that the spectrum is really a distortion of a one dimensional spectrum into a two dimensional spectrum and then a distortion of the two dimensional spectrum into a three dimensional spectrum.

No attempt has been made to analyze carefully the size

of the errors made in the calculation of $g_1(\nu)$ but the errors of Fig. 4 exceed a few percent only at a few places at most. The curve is at least as accurate as we believed anyone would ever care to know it.

5. The Complete Spectrum

As noted in Sec. 2, the total spectrum consists of three branches of which the first two are identical and have been described in the previous sections. The third branch is the same as that of a simple cubic lattice and Fig. 5 is drawn using the formulae given in Ref. 4. We wish merely to point out a few features of this spectrum that were not noted there.

The spectrum is approximately one dimensional and in contrast with the somewhat artificial application intended in Ref. 4, this appears to be a fairly realistic feature of the fibrous crystals although this is perhaps exaggerated by making $\gamma/\beta \sim 2 \times 10^{-3}$.

$g_3(\nu)$ starts at $\nu = 0$ with the characteristic ν^2 dependence

$$g_3(\nu) \sim 2\pi^{-2}\gamma^{-1}(\beta + 4\gamma)^{-\frac{1}{2}}\nu^2 \propto \nu^2 \qquad \text{for } \nu^2 \ll 2\gamma \qquad (23)$$

There are singularities at $\nu^2 = 2\gamma$ and 4γ but as ν^2 becomes larger $g(\nu)$ becomes almost equal to the one dimensional spectrum for which $g_3(\nu)$ is a constant at low frequencies

$$g_3(\nu) \sim \frac{2}{\pi} \propto \nu^0 \qquad \text{for } 4\gamma < \nu^2 \ll 1 \qquad (24)$$

These two limiting forms are shown in Fig. 5 by the broken line.

The fact that γ/β is so small makes these quantitatively accurate in contrast with some of the less accurate limiting forms for $g_1(\nu)$.

At the high frequency end of the spectrum $g_3(\nu)$ tries to become infinite as its approximate one dimensional form requires. The three dimensional form requires that $g(\nu)$ remain finite as indeed the magnified view of this end of the spectrum shows in Fig. 5.

The complete spectrum of the system is the sum of the three branches

$$g(\nu) = [2g_1(\nu) + g_3(\nu)]/3$$

Fig. 6 shows the resulting distribution by the solid curve. The broken line step function is the numerical graph obtained by S-H.

S-H recognized that the numerical calculation with a rectangular array of mesh points in the wave number space converged very slowly for computing $g_3(\nu)$. This is true not simply because of the odd shape of $g_3(\nu)$ but because of the fact that ν_3 is nearly independent of φ_1 and φ_2 and the mesh points run almost parallel with the surfaces of constant ν. Very little increase in accuracy results from taking a mesh with more than one value of (φ_1, φ_2). The accuracy depends mainly upon the number of values of φ_3 that are used. S-H did use a finer mesh for evaluating $g_3(\nu)$ than for $g_1(\nu)$ but the same difficulties also arise to a lesser extent in computing the central portion of $g_1(\nu)$ for which the surfaces of constant ν are also nearly planes.

This probably explains the apparent systematic error between $\nu \sim 0.2$ and $\nu \sim 0.6$. (The solid curve is accurate to within a fraction of a percent in most of this region.) At lower frequencies the surfaces of constant ν are much less flat and the statistical errors in the numerical scheme should be much less for $0 < \nu < 0.2$. The agreement is indeed very good in this range.

6. The Specific Heat

The specific heat at constant volume is evaluated from the equation

$$C = 3R \int_0^1 d\nu g(\nu) f(\nu T_m/T) = 3R(T/T_m) \int_0^{T_m/T} dx\, g(xT/T_m) f(x) \quad (25)$$

in which ν is still the relative frequency as used in the previous sections, $f(x)$ is the Einstein function

$$f(x) = x^2 e^x (e^x - 1)^{-2} \quad (26)$$

and

$$T_m = h\nu_m/k, \qquad x = \nu T_m/T$$

T_m is the temperature (analogous to the Debye temperature) associated with the maximum frequency ν_m, for which $\nu = 1$.

For low temperatures, $T \ll T_m$, only the low frequency modes, $\nu \ll 1$, contribute appreciably to C. Since the function $f(x)$ decreases rapidly for $x \gg 1$ the main contribution to Eq. (25) comes from values of x of order 1 and

$$C \sim 3R(T/T_m) \int_0^\infty dx\, g(xT/T_m) f(x) \qquad \text{for } T \ll T_m \quad (25a)$$

If for small values of $\nu = xT/T_m$, $g(\nu)$ should be proportional to ν^ℓ for some value of ℓ, i.e., $g(\nu) = A\nu^\ell$, then

$$C \sim 3RA(T/T_m)^{\ell+1} \int_0^\infty dx\, x^\ell f(x) = 3RA\Gamma(\ell+3)\zeta(\ell+2)(T/T_m)^{\ell+1} \tag{27}$$

$$\propto T^{\ell+1}$$

$\zeta(\ell+2)$ is the Riemann zeta-function.

It is convenient to consider separately the contribution to C from the branches $g_1(\nu) = g_2(\nu)$ and $g_3(\nu)$ by writing

$$C = (2C_1 + C_3)/3 \tag{28}$$

for which C_1 is the contribution to C from the branch $g_1(\nu)$ and C_3 the contribution from $g_3(\nu)$.

For $\nu^2 \ll \gamma^2/4\varkappa$, $g_1(\nu)$ is proportional to ν^2, Eq. (8), and for $\nu^2 \ll \gamma$, $g_3(\nu)$ is also proportional to ν^2, Eq. (23). In the range x of order one, $\nu = xT/T_m \ll \gamma/\sqrt{4\varkappa}$ if $T \ll T_m\,\gamma/\sqrt{4\varkappa}$ and so we find that

$$C_1 \sim \frac{4R\pi^2(T/T_m)^3}{5\gamma(\alpha+4\gamma)^{\frac{1}{2}}} \propto T^3 \qquad \text{for } T \ll T_m\,\gamma/\sqrt{4\varkappa} \ll T_m \tag{29}$$

and similarly

$$C_3 \sim \frac{4R\pi^2(T/T_m)^3}{5\gamma(\beta+4\gamma)^{\frac{1}{2}}} \propto T^3 \qquad \text{for } T \ll T_m\sqrt{\gamma} \ll T_m \tag{30}$$

C as well as its two components individually is proportional to T^3 for sufficiently low T in agreement with the familiar Debye T^3-law except that, in the present case, the T^3

behavior extends over only a relatively very short range of T; for a typical three dimensional system the T^3 behavior is limited only by $T \ll T_m$ i.e., for temperatures small compared with the Debye temperature.

From Eq. (9) we see that $g_1(\nu)$ is proportional to $\nu^{3/2}$ for $\gamma^2/4\varkappa \ll \nu^2 \ll \gamma$. If $\gamma/\varkappa$ is sufficiently small, the $\nu^{3/2}$ dependence holds over almost the entire range $\nu^2 \ll \gamma$, except for a very small region near $\nu = 0$. C_1 represents an average of contributions from all values of $\nu = xT/T_m$ with $x = O(1)$. If $T_m\gamma/\sqrt{4\varkappa} \ll T \ll T_m\sqrt{\gamma}$, then $g(\nu) \propto \nu^{3/2}$ for most values of ν that contribute to C_1 and we find that

$$C_1 \sim \frac{315R(T/T_m)^{5/2}\zeta(7/2)}{8\pi^{3/2}\gamma^{1/2}(\alpha + 4\gamma)^{1/2}\varkappa^{1/4}} \propto T^{5/2} \quad \text{for } T_m\gamma/\sqrt{4\varkappa} \ll T \ll T_m\sqrt{\gamma} \tag{31}$$

The $T^{5/2}$ dependence of the specific heat is not a consequence of geometry and the $\nu^{3/2}$ dependence was one of the better approximations in the analysis if $g_1(\nu)$. At least a trend in this direction should appear for any fibrous crystal. If one should plot C_1 vs. T on a log-log scale, the curve should have a slope 3 at the lowest values of T and show a range of T over which the curve is rather flat with a slope of 5/2.

One does not, of course, measure C_1 experimentally but only C and in this range of T, we expect C_3 to be proportional to T^3 still. The total specific heat would be a linear combination of T^3 and $T^{5/2}$ and the log-log plot of C would have a

slope intermediate between 3 and 5/2, nearer the 5/2, however, because at these temperatures C_1 would be appreciably larger than C_3.

For this particular model, we would find also, by quite similar arguments, a range of T for which

$$C_1 \sim \frac{45R(T/T_m)^{3/2}[\Gamma(1/4)]^2\zeta(5/2)}{16\pi^2\alpha^{1/2}\varkappa^{1/4}} \propto T^{3/2} \quad \text{for } \sqrt{\gamma}\, T_m \ll T \ll \sqrt{\alpha}\, T_m \tag{32}$$

due to the $\nu^{1/2}$ dependence of $g_1(\nu)$ given in Eq. (12). This behavior of $g_1(\nu)$ was a limiting form that did not show too well for the force constants used here and furthermore it was primarily a consequence of the rectangular geometry. The specific heat being an average of contributions from a wide range of ν, would not be expected to show this behavior even as accurately as $g_1(\nu)$ showed the $\nu^{1/2}$ dependence. The $T^{3/2}$ represents only a trend peculiar to the geometry.

Also from Eq. (14) which gives $g_1(\nu) \propto \nu^{-1/2}$ we obtain

$$C_1 \sim \frac{9R(T/T_m)^{1/2}\zeta(3/2)}{2^{5/2}\pi^{1/2}\varkappa^{1/4}} \propto T^{1/2} \quad \text{for } \sqrt{\alpha}\, T_m \ll T \ll \sqrt{4\varkappa} \tag{33}$$

This is expected to be only a rather crude approximation as was Eq. (14) because it requires $\sqrt{4\varkappa/\alpha} \gg 1$. This dependence was not mainly a consequence of geometry, however and we can expect this sort of temperature dependence to be approximately true for any fibrous structure.

Returning to the behavior of C_3 we see also from Eq. (24) that

$$C_3 \sim \tfrac{1}{2} R\pi^3 (T/T_m) \propto T \qquad \text{for } 2\sqrt{\gamma}\, T_m \ll T \ll T_m \qquad (34)$$

This behavior is not mainly a consequence of geometry but of the fact that the central forces in the chain are very strong.

In a crude sort of way, we can eliminate the effects of the geometry by making γ of the same order of magnitude as α. The features to be expected of any fibrous structure are that

$$C_1 \propto T^3 \qquad \text{for } T \ll T_m\, \alpha/\sqrt{4\varkappa}$$

$$C_1 \propto T^{5/2} \qquad \text{for } T_m\, \alpha/\sqrt{4\varkappa} \ll T_m \ll \sqrt{\alpha}\, T_m$$

$$C_1 \propto T^{1/2} \qquad \text{for } T_m \sqrt{\alpha} \ll T_m \ll T_m \sqrt{\varkappa}$$

and

$$C_3 \propto T^3 \qquad \text{for } T \ll \sqrt{\alpha}\, T_m$$

$$C_3 \propto T \qquad \text{for } \sqrt{\alpha}\, T_m \ll T \ll T_m$$

in which $\gamma = \alpha$ represents a qualitative measure of the forces between the chains.

Acknowledgments

The authors would like to thank Professor W. Stockmayer for lending a copy of Mr. Hecht's thesis which gave a more detailed account of their work.

Appendix

In Sec. 4, it has been shown that several new types of singularities can arise in idealized situations in which valence forces resisting the bending of bond angles are a dominant influence on the spectrum. For the model considered here, these arise from the term $\varkappa(1 - \cos \varphi_3)^2$ which is approximately $(\varkappa/4)\varphi_3^4$ for $\varphi_3 \ll 1$. Near any critical frequency on the face $\varphi_3 = 0$, the dependence of ν on the wave numbers was described by an equation of the form of Eq. (20), i.e.,

$$\nu^2 = \nu_c^2 + a(\varphi_1 - \varphi_{1c})^2 + b(\varphi_2 - \varphi_{2c})^2 + c(\varphi_3 - \varphi_{3c})^4 \quad \text{(A1)}$$

Various kinds of singularities arose in $g(\nu)$ depending upon whether a, b and c were zero, positive or negative.

Table II contains a list of all the various possibilities with $c \neq 0$. If $c = 0$, Eq. (A1) reduces to a two dimensional quadratic form giving singularities in $g(\nu)$ of a type already considered by van Hove. Of the 18 anomalous singularities listed, many combine into equivalent pairs because the form of Eq. (A1) is invariant to interchange of a and b along with an interchange of dummy indices 1 and 2 on φ_1 and φ_2, thus $a < 0$, $b > 0$ is equivalent to $a > 0$, $b < 0$. Furthermore if we change the sign of a, b and c, this is equivalent to changing $\nu^2 - \nu_c^2$ to $\nu_c^2 - \nu^2$. The 18 cases can be grouped into pairs differing only in that $\nu > \nu_c$ for one of the pairs is equivalent to $\nu < \nu_c$ for the other. A minimum is paired with a maximum, for example.

Table II. All possible types of anomalous singularities are classified according to whether a, b and c are positive (+), negative (-) or zero (0). The fourth column indicates that the singularity is a one, two or three dimensional form (1D, 2D or 3D) of a minimum (min.), maximum, (max.) or saddle point (S.P.). The fifth column indicates the approximate frequency at which any of these types appear in Fig. 4 (see Sec. 4).

a	b	c	type	ν^2
0	0	+	1D min.	0
0	0	-	1D max.	
0	+	+	2D min.	0
+	0	+		
0	-	-	2D max.	
-	0	-		
0	+	-	2D SPI	
+	0	-		
0	-	+	2D SPII	
-	0	+		α
+	+	+	3D min.	0
-	-	-	3D max.	
+	+	-	3D SPI	
-	-	+	3D SPII	$\alpha + 4\gamma$
+	-	+	3D SPIII	2γ
-	+	+		$\alpha + 2\gamma$
+	-	-	3D SPIV	
-	+	-		

Except for these differences due to interchange of φ_1 and φ_2 or reflections of the frequency about ν_c, there are only six different kinds of singularities as grouped in Table II, one one dimensional case, two two dimensional cases, and three three dimensional cases. The present model conveniently displays, at least approximately, an example of each of the six types, always a case with $c > 0$ (it is hard to imagine how $c < 0$ could ever arise in a practical problem except by accident). The model also shows all of the standard kinds of singularities described by van Hove for three dimensional lattices and approximately all the usual kinds of singularities for one and two dimensional lattices as well.

Critical wave numbers and frequencies of anomalous types are to be expected in quite general chain polymer crystals in which the dominant forces resisting displacements perpendicular to the chain result from the bending of bond angles. This does not, however, exhaust all the possible kinds of anomalous singularities of physical interest. A somewhat similar situation arises in layer type crystals such as graphite[2]. The forces resisting displacements perpendicular to the crystal planes for the lamellar crystals seem to arise also mainly from the bending of bond angles but now the fourth power dependence of ν^2 on wave numbers is associated with two of the three wave number components instead of just one as for the chain polymer crystals.

Corresponding to Eq. (A1), we might obtain for the lamellar crystals critical points for which

$$\nu^2 \sim \nu_c^2 + a(\varphi_1 - \varphi_{1c})^4 + b(\varphi_1 - \varphi_{1c})^4 + c(\varphi_3 - \varphi_{3c})^2 \quad (A2)$$

Actually one is apt to obtain a more general form

$$\nu^2 \sim \nu_c^2 + a(\theta)\varphi^4 + c(\varphi_3 - \varphi_{3c})^2 \quad (A3)$$

in which θ and φ are the polar representations of $\varphi_1 - \varphi_{1c}$ and $\varphi_2 - \varphi_{2c}$,

$$\varphi_1 - \varphi_{1c} \equiv \varphi \cos \theta, \quad \varphi_2 - \varphi_{2c} \equiv \varphi \sin \theta.$$

$a(\theta)$ is some continuous function of θ but not necessarily that implied by Eq. (A2) and φ_3 can correspond to any arbitrary direction in the wave number space but in practical situations would almost certainly be the wave number component for waves traveling perpendicular to the crystal planes of the lamellar structure.

There are not many new types of singularities arising from Eqs. (A2) or (A3) that are of general interest. If either $a = 0$ or $b = 0$ in Eq. (A2), the form of Eq. (A2) reduces to a special case of Eq. (A1). No physical situation comes to mind that would give negative values for a or b and, in fact, the lamellar crystals are expected to lead to equations such as Eq. (A3) with $a(\theta)$ positive definite. There are, however, still three kinds of singularities that are certain to arise in limiting cases of physically realistic situations, namely $a(\theta) > 0$ and $c > 0$ (a three dimensional minimum), $c < 0$ (a three dimensional saddle point) and $c = 0$ (a two dimensional minimum). Examples of each of these appear in the spectrum of

graphite proposed by Komatsu and Nagamiya[7].

There finally is the possibility that ν^2 could be proportional to the fourth power of the wave number components in all three directions, i.e., ν^2 a homogeneous fourth degree polynomial in the $(\varphi_j - \varphi_{jc})$. It is difficult to imagine any physical situation that would give rise to this, however.

We shall consider here only the nine physically interesting cases mentioned above, the six in Table II and the three special cases of Eq. (3A). Without loss of generality, we may assume the φ_1, φ_2 and φ_3 are any three independent wave vector components scaled in such a way that ν^2 is periodic in φ_1, φ_2 and φ_3 with period 2π. The normalized distribution density of ν^2 (for any individual branch of the spectrum) $G(\nu^2)$ is defined by

$$G(\nu^2) = (2\pi)^{-3} \frac{d}{d\nu^2} \iiint d\varphi_1 d\varphi_2 d\varphi_3 \qquad \text{(A4)}$$

integrated over the region

$$\nu^2(\varphi_1, \varphi_2, \varphi_3) < \nu^2, \quad 0 < \varphi_j < 2\pi$$

Even though the value of $G(\nu^2)$ does not, in most cases, depend only upon the local behavior of ν^2 $(\varphi_1, \varphi_2, \varphi_3)$ near $\varphi_j = \varphi_{jc}$, the singular properties of $G(\nu^2)$ in which we are interested are a consequence of the local properties and we may consider the various cases of Table II as if Eq. (A1) were valid for all values of the φ_j's. Either of two things may happen as $\nu^2 \longrightarrow \nu_c^2$. If $G(\nu^2) \longrightarrow \infty$ as $\nu^2 \longrightarrow \nu_c^2$, then the value of $G(\nu^2)$ as $\nu^2 \longrightarrow \nu_c^2$ is dominated by the contributions from the

neighborhood of the critical wave vector where Eq. (A1) is accurate. If $G(\nu_c^2)$ is finite, its value will, in most cases, depend upon properties of ν^2 $(\varphi_1, \varphi_2, \varphi_3)$ far away from the critical wave vector where Eq. (A1) is not accurate. If, however, we evaluate $G(\nu^2) - G(\nu_c^2)$ using the same approximations, Eq. (A1), in evaluating each term, the contributions far from the critical point nearly cancel and we can still correctly determine the kind of singularity from the behavior of $G(\nu^2) - G(\nu_c^2)$ even though we cannot find either $G(\nu^2)$ or $G(\nu_c^2)$ individually.

From Eq. (A1), we notice that ν^2 is locally an even function of $(\varphi_j - \varphi_{jc})$ for $j = 1, 2$, and 3 so that the contribution to $G(\nu^2)$ from the vicinity of the critical wave vector is eight times that from the region $(\varphi_j - \varphi_{jc}) > 0$. If we consider $c > 0$, which can be done with no loss of generality, the range of $\varphi_3 > 0$ in Eq. (A4) is

$$0 < \varphi_3 < c^{-\frac{1}{4}}[\nu^2 - \nu_c^2 - a(\varphi_1 - \varphi_{1c})^2 - b(\varphi_2 - \varphi_{2c})^2]^{\frac{1}{4}}$$

and so

$$G(\nu^2) \sim \tfrac{1}{4}\pi^{-3}c^{-\frac{1}{4}} \iint [\nu^2 - \nu_c^2 - a(\varphi_1 - \varphi_{1c})^2 - b(\varphi_2 - \varphi_{2c})^2]^{-3/4}\, d\varphi_1 d\varphi_2 \qquad (A5)$$

The limits of integration are automatically taken care of by the requirement that the integrand be real, i.e., the quantity in brackets must be positive and also

$$0 < \varphi_j - \varphi_{jc} < M_j, \quad j = 1, 2, 3. \qquad (A6)$$

M_j is some number of order 1. If a = 0 (ν^2 independent of φ_1) we must choose $M_1 = \pi$ and if b = 0 (ν^2 independent of φ_2) we must take $M_2 = \pi$. Except for these cases, the actual value of M_j is unimportant because Eqs. (A1) and (A5) are only approximations valid for $|\varphi_j - \varphi_{jc}| << 1$. Any results that are meaningful can not involve the values of M_j for this would immediately imply that the results depended upon the behavior of $\nu^2(\varphi_1, \varphi_2, \varphi_3)$ in a region where Eq. (A1) is incorrect.

The one dimensional result (a = 0, b = 0) follows directly from Eq. (A5)

$$G(\nu^2) \sim \begin{cases} 0 & \text{for } \nu^2 < \nu_c^2 \\ (\nu^2 - \nu_c^2)^{-3/4}/4\pi c^{1/4} & \text{for } \nu^2 > \nu_c^2 \end{cases} \tag{A7}$$

with $G(\nu^2) \to \infty$ as $\nu^2 \to \nu_c^2$.

For the two dimensional cases (b = 0), we make the substitution

$$x = |a(\varphi_1 - \varphi_{1c})^2/(\nu^2 - \nu_c^2)|^{1/2} \tag{A8}$$

and obtain the following limiting expressions. For a < 0 (2D min.),

$$G(\nu^2) = 0 \qquad \text{for } \nu^2 < \nu_c^2 \tag{A9a}$$

$$G(\nu^2) \sim \frac{(\nu^2 - \nu_c^2)^{-\frac{1}{4}}}{4\pi^2 |a|^{\frac{1}{4}} c^{\frac{1}{4}}} \int_0^1 \frac{dx}{(1 - x^2)^{3/4}}$$

$$= \frac{(\nu^2 - \nu_c^2)^{-\frac{1}{4}} [\Gamma(1/4)]^2}{8\pi^2 |2\pi a|^{\frac{1}{4}} c^{\frac{1}{4}}} \qquad \text{for } \nu^2 > \nu_c^2 \tag{A9b}$$

Again $G(\nu^2) \to \infty$ as $\nu^2 \to \nu_c^2$. For a > 0 (2D SP)

$$G(\nu^2) \sim \begin{cases} \dfrac{|\nu^2 - \nu_c^2|^{-\frac{1}{4}}[\Gamma(1/4)]^2}{8\pi^2|\pi a|^{\frac{1}{2}}c^{\frac{1}{4}}} + C & \text{for } \nu^2 < \nu_c^2 \\ \dfrac{|\nu^2 - \nu_c^2|^{-\frac{1}{4}}[\Gamma(1/4)]^2}{8\pi^2|2\pi a|^{\frac{1}{2}}c^{\frac{1}{4}}} + C & \text{for } \nu^2 > \nu_c^2 \end{cases} \tag{A10}$$

in which C is some undetermined constant.

The three dimensional cases with a and b of the same sign, (±), can be conveniently handled by a polar coordinate substitution

$$|a|^{\frac{1}{2}}(\varphi_1 - \varphi_{1c}) \equiv r\cos\theta, \quad |b|^{\frac{1}{2}}(\varphi_2 - \varphi_{2c}) \equiv r\sin\theta$$

which transforms Eq. (A5) into

$$G(\nu^2) \sim \frac{1}{8\pi^2|ab|^{\frac{1}{2}}c^{\frac{1}{4}}} \int \frac{r\,dr}{[\nu^2 - \nu_c^2 \mp r^2]^{3/4}}$$

This gives immediately the results for a, b > 0 (3D min.)

$$G(\nu^2) \sim \begin{cases} 0 & \text{for } \nu^2 < \nu_c^2 \\ \dfrac{(\nu^2 - \nu_c^2)^{\frac{1}{4}}}{4\pi^2|ab|^{\frac{1}{2}}c^{\frac{1}{4}}} & \text{for } \nu^2 > \nu_c^2 \end{cases} \tag{A11}$$

and for a, b < 0 (3D SPII)

$$G(\nu^2) - G(\nu_c^2) \sim \begin{cases} 0 & \text{for } \nu^2 < \nu_c^2 \\ \dfrac{-(\nu^2 - \nu_c^2)^{\frac{1}{4}}}{4\pi^2|ab|^{\frac{1}{2}}c^{\frac{1}{4}}} & \text{for } \nu^2 > \nu_c^2 \end{cases} \tag{A12}$$

Both Eqs. (A11) and (A12) give verticle tangents on only one side of ν_c^2.

The remaining singularity, a > 0, b < 0 (3D, SPIII) gives

$$G(\nu^2) - G(\nu_c^2) \sim \begin{cases} -\dfrac{|\nu^2 - \nu_c^2|^{\frac{1}{4}}}{2^{3/2}\pi^2|ab|^{\frac{1}{2}}c^{\frac{1}{4}}} & \text{for } \nu^2 < \nu_c^2 \\ -\dfrac{|\nu^2 - \nu_c^2|^{\frac{1}{4}}}{4\pi^2|ab|^{\frac{1}{2}}c^{\frac{1}{4}}} & \text{for } \nu^2 > \nu_c^2 \end{cases} \tag{A13}$$

which has a (asymmetric) verticle tangent singularity on both sides of ν_c^2.

For the three interesting cases arising from Eq. (A3), we let

$$A \equiv \tfrac{1}{4}\pi^{-2}\int_0^{\pi/2} d\theta[a(\theta)]^{-1/2} \tag{A14}$$

and obtain the following expressions. For c = 0 (2D min.)

$$G(\nu^2) = \begin{cases} 0 & \text{for } \nu^2 < \nu_c^2 \\ A(\nu^2 - \nu_c^2)^{-1/2} & \text{for } \nu^2 > \nu_c^2 \end{cases} \tag{A15}$$

which has an infinite singularity. For c > 0 (3D min.)

$$G(\nu^2) = \begin{cases} 0 & \text{for } \nu^2 < \nu_c^2 \\ \tfrac{1}{2}\pi^{-1}c^{-1/2}A & \text{for } \nu^2 > \nu_c^2 \end{cases} \tag{A16}$$

a finite discontinuity. For c < 0 (3D SP)

$$G(\nu^2) = C - \pi^{-1}|c|^{-1/2} A \log|\nu^2 - \nu_c^2| \tag{A17}$$

another infinite singularity. C is again an undetermined constant.

Figure Captions

Fig. 1. Three dimensional surfaces of constant frequency in the wave number space (φ_1, φ_2, φ_3) for modes vibrating perpendicular to the chains are shown for several small values of ν. For the smallest ν, the surfaces are ellipses flat in the φ_1 direction. Due to the valence forces, the surfaces become elongated in the φ_2 direction for the larger values of ν.

Fig. 2. Three dimensional surfaces of constant frequency for larger values of ν are shown by their intersections with the planes φ_1, φ_2 and $\varphi_3 = 0$ or π. Solid lines are intersections with the faces $\varphi_j = \pi$, broken lines with the faces $\varphi_3 = 0$, of the cube, $j = 1$, 2 or 3. The surfaces are labeled with the values of ν^2. For small ν^2, the surfaces are elliptical shaped near the origin, see Fig. 1, become elongated in the φ_2 direction as ν^2 increases, become nearly cylindrical for $2\gamma < \nu^2 < \alpha$. For $\alpha + 4\gamma < \nu^2 < 4\varkappa$, the surfaces are nearly planes perpendicular with the φ_3 axis. The largest ν^2, $4\varkappa + \alpha + 2\gamma$, is at the point $(\pi, 0, \pi)$.

Fig. 3. $g_1(\nu)$, the frequency distribution for modes vibrating perpendicular to the chains, plotted for small values of ν, show the transition from $g(\nu) \propto \nu^2$ to $g(\nu) \propto \nu^{3/2}$. Curve (1) is proportional to ν^2, Eq. (8); curve (2) is proportional to $\nu^{3/2}$, Eq. (9), and curve 3 is the accurate curve for $g(\nu)$, Eq. (10).

Fig. 4. A plot of $g_1(\nu)$ for the complete range of ν, Fig. 3, is a magnified view of the small rectangle near the origin. The solid curve shows an accurate curve of $g_1(\nu)$. The three broken curves, proportional to $\nu^{3/2}$, $\nu^{1/2}$ and $\nu^{-1/2}$ represent Eqs. (9), (12) and (14), respectively.

Fig. 5. $g_3(\nu)$, the spectrum for modes vibrating parallel with the chains, is plotted for the entire range of ν with a magnified view of the high frequency end shown by the insert. The broken curves are proportional to ν^2 and ν^0 = const., $2/\pi$, corresponding to Eqs. (23) and (24), respectively.

Fig. 6. The complete frequency distribution for all modes, $g(\nu)$, is shown by the solid curve. The step function curve is the approximate curve computed by Stockmayer and Hecht for the same system.

References

1. A few of the recent contributions are:
   W. De Sorbo and W. W. Tyler, J. Chem. Phys. 21, 1660 (1953)
   Dworkin, Sasmor and Van Artsdalen, J. Chem. Phys. 22, 837 (1954)
   Bergenlid, Hill, Webb, and Wilks, Phil. Mag. 45, 851 (1954)
   P. H. Keesom and N. Pearlman, Phys. Rev. 99, 1119 (1955).
2. Some recent contributions are:
   J. Krumhansl and H. Brooks, J. Chem. Phys. 21, 1663 (1953)
   T. Nagamiya and K. Komatsu, J. Chem. Phys. 22, 1457 (1954)
   K. Komatsu J. Phys. Soc. Japan 10,346(1955)
   G. F. Newell J. Chem. Phys. 23, 2431 (1955)
   J. Chem. Phys. 24 (1956).
3. W. H. Stockmayer and C. E. Hecht, J. Chem. Phys. 21, 1954 (1953) hereafter denoted as S-H.
4. G. F. Newell J. Chem. Phys. 21, 1877 (1953).
5. L. van Hove Phys. Rev. 89, 1189 (1953)
   E. W. Montroll Amer. Math. Monthly 61, 46(1954.
6. This corresponds to S-H Eq. (3.4) except that there seems to be an error in this equation. $I_1 = I_2$ should be replaced by $I_1 + I_2$ and I_3 by $I_3/2$.
7. K. Komatsu and T. Nagamiya, J. Phys. Soc. (Japan) 6, 438 (1951).

Fig 1.

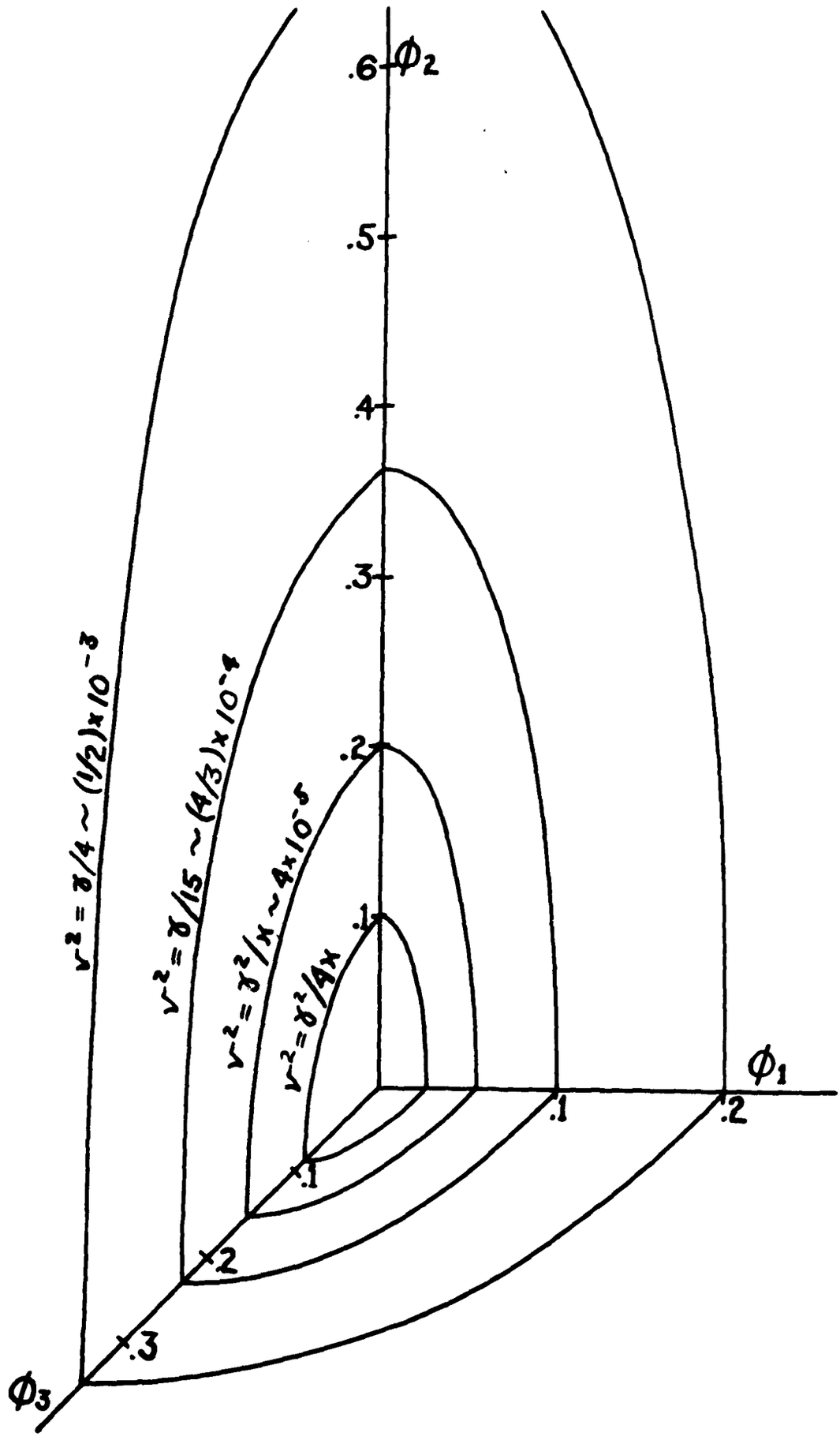
.6 ϕ_2
.5
.4
.3
.2
.1
ϕ_1
.1
.2
.1
.2
.3
ϕ_3
$r^2 = \gamma/4 \sim (1/2)\times 10^{-3}$
$r^2 = \gamma/15 \sim (4/3)\times 10^{-4}$
$r^2 = \gamma^2/N \sim 4\times 10^{-5}$
$r^2 = \gamma^2/4N$

Fig 2.

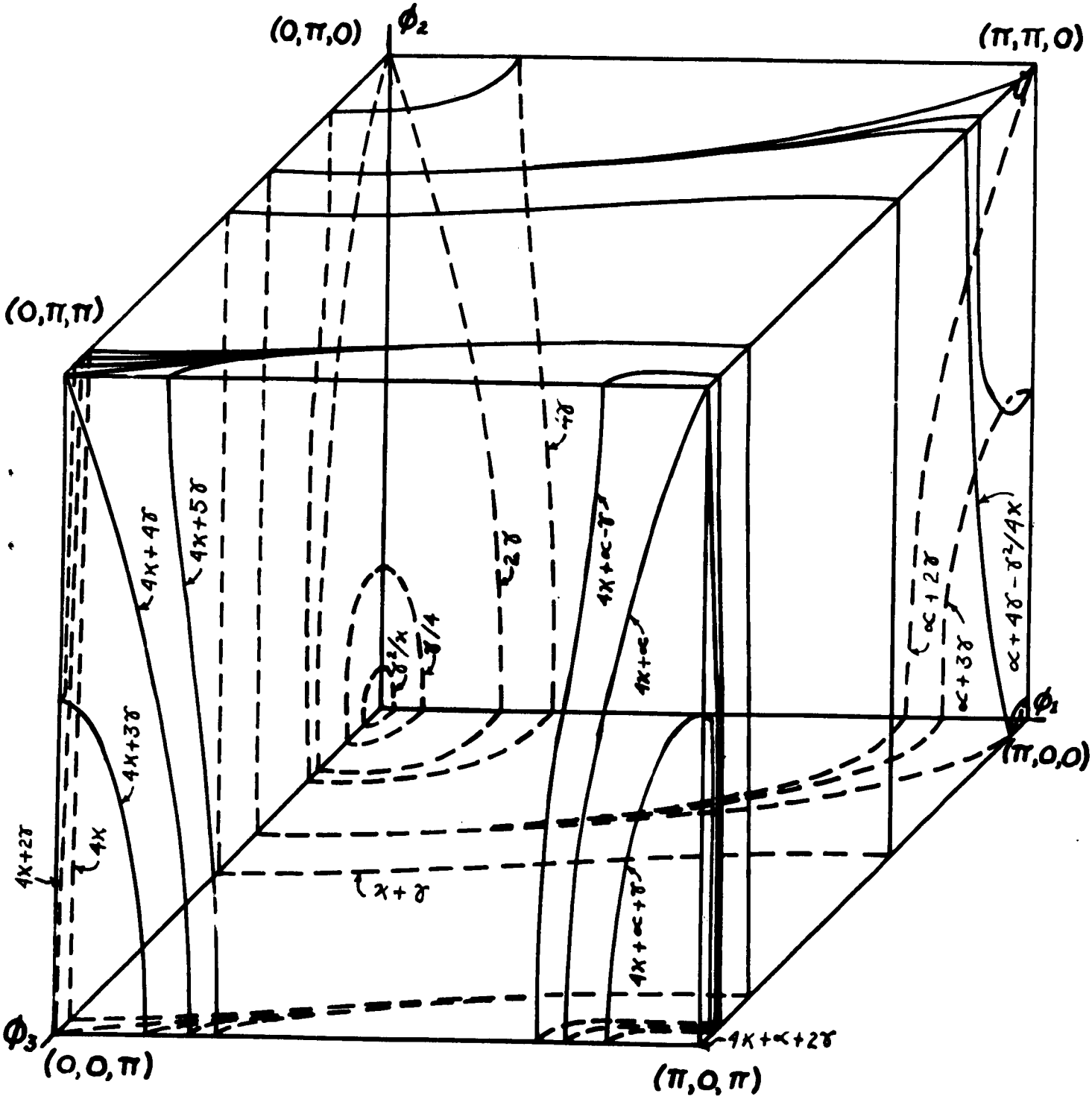
(0,π,0)
ϕ_2
(π,π,0)
(0,π,π)
4x+4δ
4x+5δ
τ+δ
τ+2δ
4x+α-δ
4x+α
α+2δ
α+3δ
α+4δ-δ²/4x
ϕ_1
(π,0,0)
4x+3δ
4x+2δ
4x
τ+δ
4x+α+δ
ϕ_3
(0,0,π)
4x+α+2δ
(π,0,π)

Fig. 3

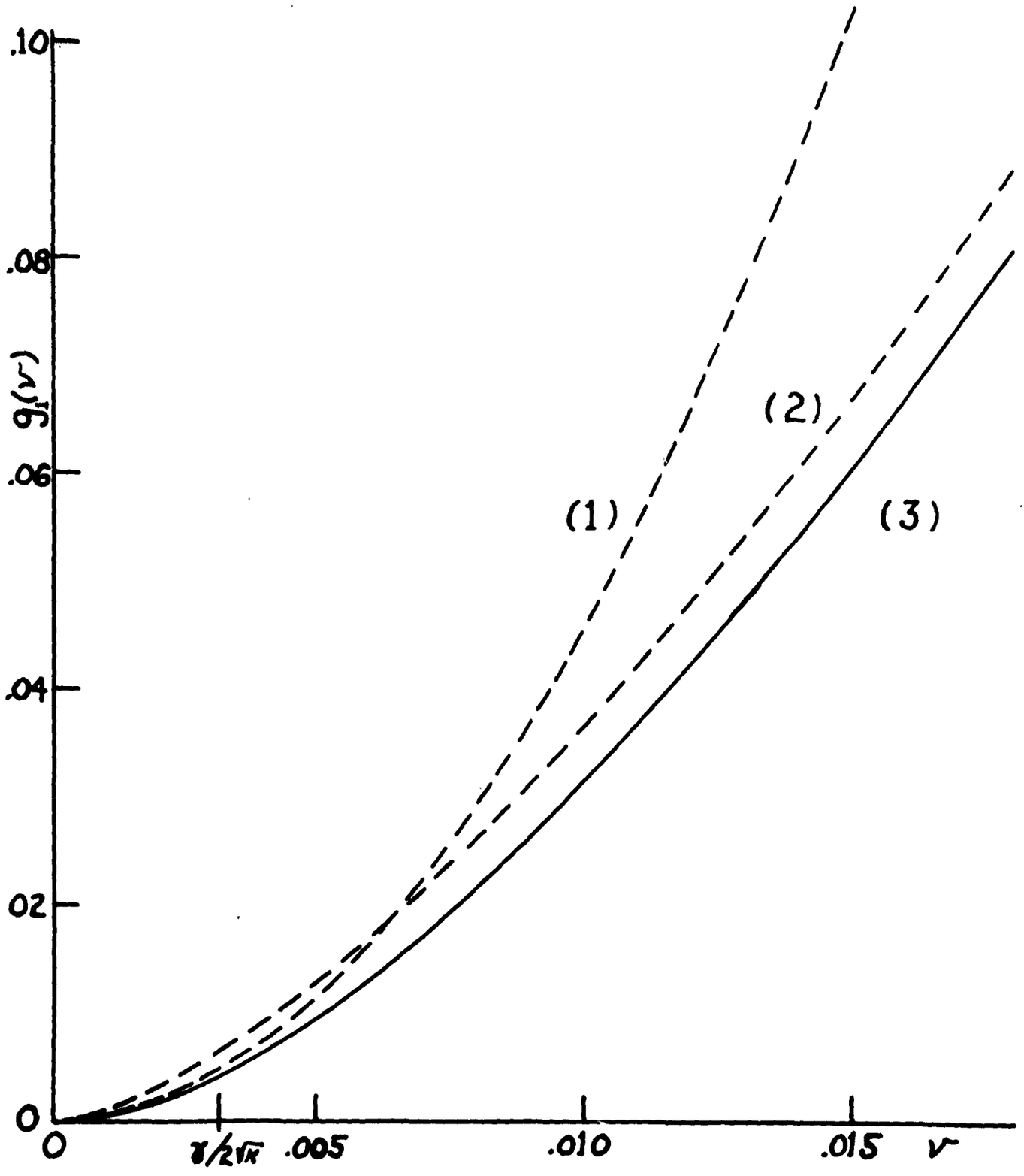

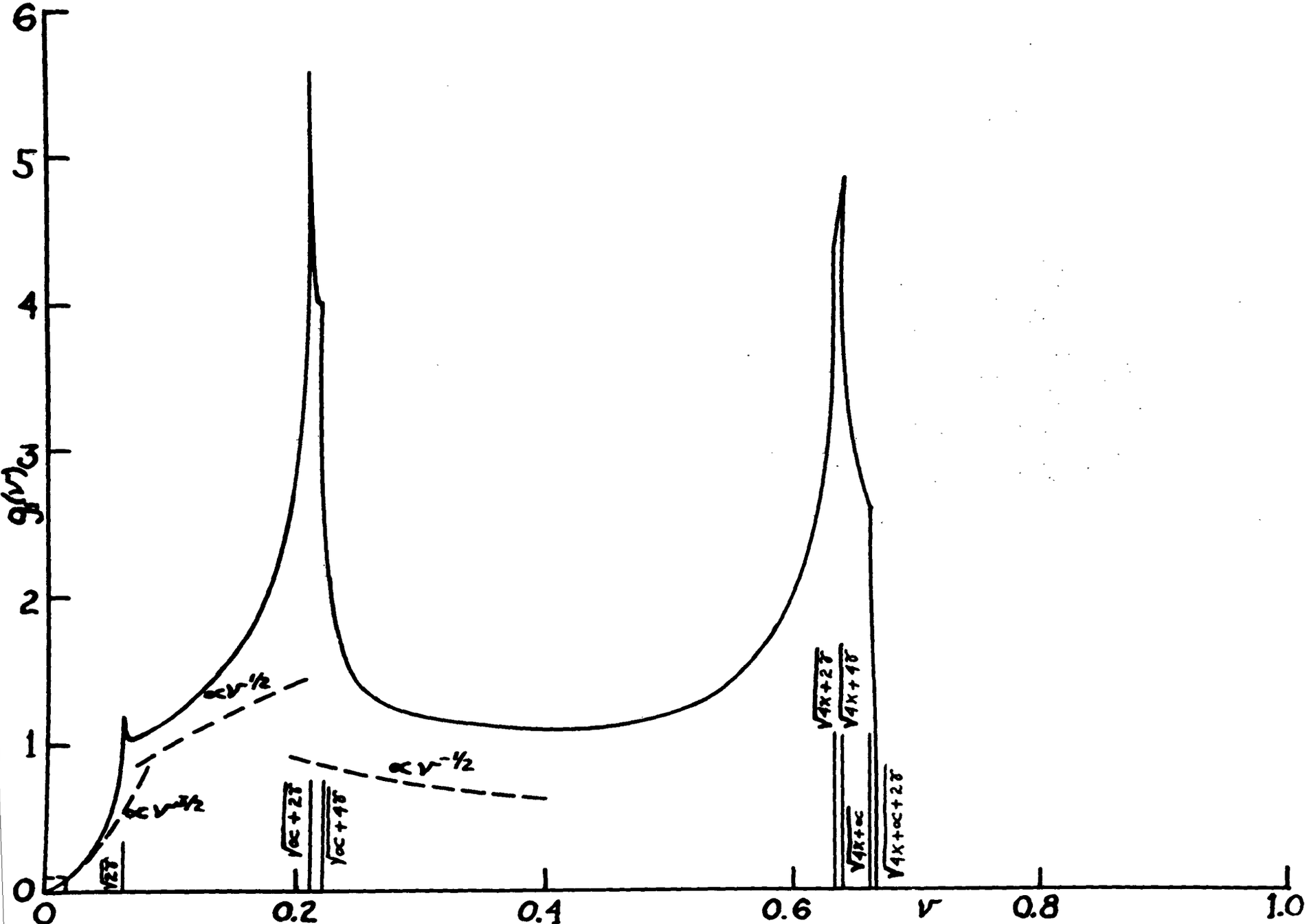
6
5
4
2
1
0
$g(\nu)_{CM}$
$\propto \nu^{1/2}$
$\propto \nu^{3/2}$
$\propto \nu^{-1/2}$
$\sqrt{2\alpha}$
$\sqrt{2\alpha+2\beta}$
$\sqrt{2\alpha+4\beta}$
$\sqrt{4\alpha}$
$\sqrt{4\alpha+2\beta}$
$\sqrt{4\alpha+4\beta}$
$\sqrt{4\alpha+\alpha c}$
$\sqrt{4\alpha+\alpha c+2\beta}$
0
0.2
0.4
0.6
ν
0.8
1.0

Fig. 4

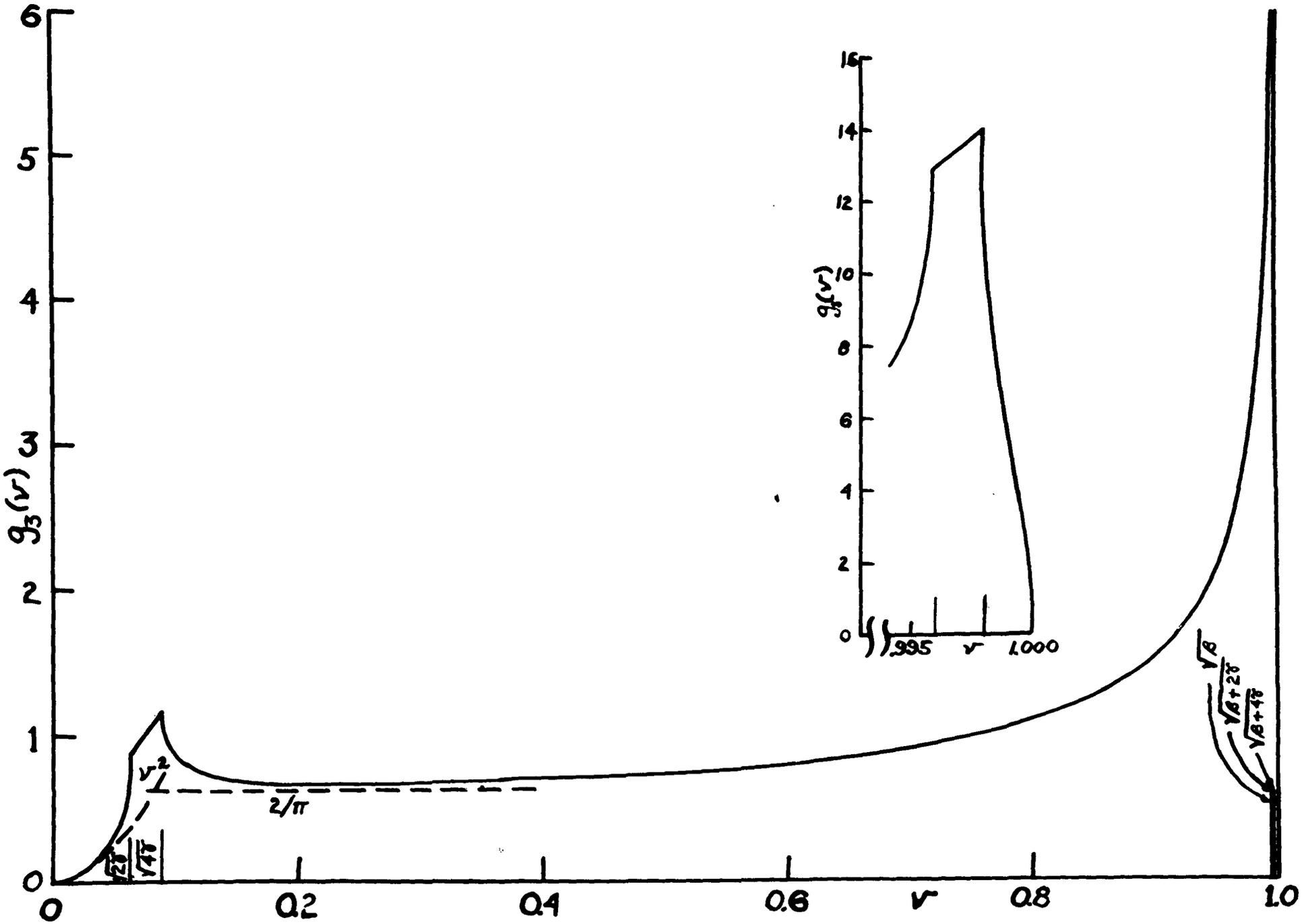
6
5
4
3
2
1
0
$g_3(v)$
0
0.2
0.4
0.6
0.8
1.0
v
v^2
$2/\pi$
$\sqrt{2\delta}$
$\sqrt{4\delta}$
$\sqrt{\delta}$
$\sqrt{\delta+2\delta}$
$\sqrt{\delta+4\delta}$
16
14
12
10
8
6
4
2
0
$g_3(v)$
.995
v
1.000

Fig. 5.

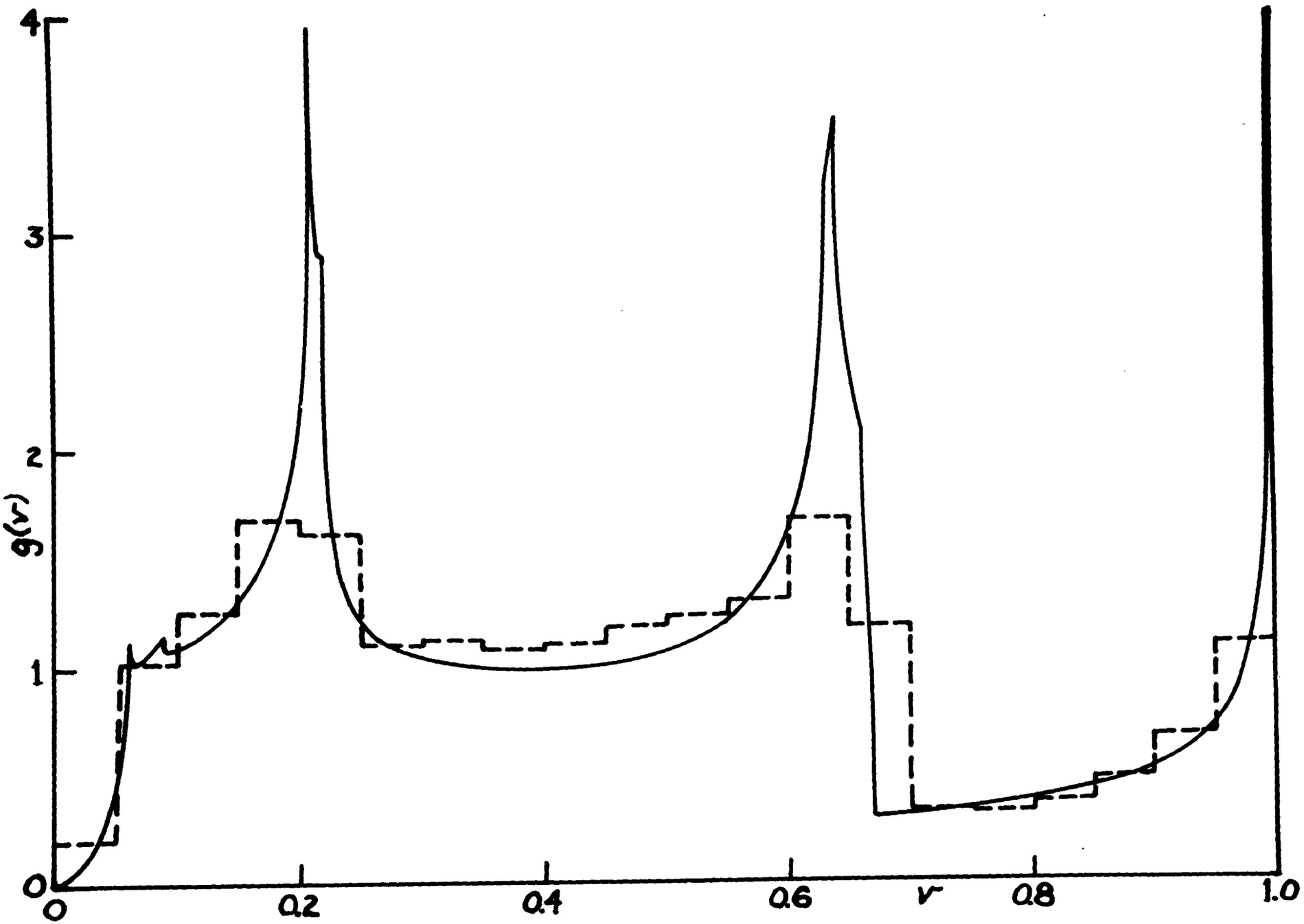

Fig. 6